

A GENERAL MODEL OF LATERAL WEB DYNAMICS BETWEEN TWO REELS

By

Sinan Müftü and Hankang Yang
Northeastern University
USA

ABSTRACT

A flexible web unavoidably deviates from its prescribed (linear) path during processing. The lateral web dynamics can be caused by tilt of rollers, web defects, off axis motion of the reels and other factors. In this work we present a generalized model of web transport between two reels, supported by numerous rollers. The mechanics of the web between the two reels is represented by a single partial differential equation, hence coupling of web-spans or lack thereof can be predicted. Web-to-roller interaction is modeled by assuming that tape sticks to the roller surface. The results of this general model are compared to the well-known model by Shelton and Reid (SR), which is applicable in the free span between two rollers. Good agreement between the present model and SR-model is found when the upstream free-span is stiff (or the downstream free-span is compliant), when the wrap angle is large and lateral bending rigidity is high. The present model otherwise predicts coupling of the mechanics of the free spans. The model is flexible to consider a variety of imperfections related to the web geometry and the path components. The lateral motion of a weaved web which is transported on a path with tilted rollers is simulated. The amplitude and the direction of the scatter wind due to this effect are predicted. In general the model shows that the coupling between the upstream and downstream web spans around a roller should not be neglected.

NOMENCLATURE

α	Orientation angle of roller axis
δ	Tilt of roller axis
λ_w	Wave length of the weave imperfection
ν	Poisson's ratio
Ω	Roller spin velocity
ρ	Web density
θ	Tape position on the roller

θ_g	Slope of the roller centerline with respect to ideal tape path, x .
θ_w	Wrap angle of the web over a roller
A_w	Amplitude of the weave imperfection
b	Web width
Dw/Dt	Material time derivative (= $w_{,t} + V_x w_{,x}$)
E	Elastic modulus
h	Web thickness
H_i	Window function (= 1 over the roller, = 0 otherwise)
i	Subscript denoting the roller number
I	2 nd moment of area
L_1	Length of web upstream of the roller
L_2	Length of tape wrapped around the roller
L_3	Length of web downstream of the roller
N_r	Number of rollers on the path
R	Radius of roller
T	Tension
V_x	Web transport speed
w_g	Shape of the roller with respect to the ideal tape path, x .
w_0	Weave imperfection
w	
x_{1-3}	Reference roller coordinates
x'_{1-3}	Deflected roller coordinates

INTRODUCTION

Thin substrates used in various industries and manufacturing processes ranging from data recording tape, to food-wrap, to flexible-electronics are collectively known as webs. In a typical web handling process a web travels between two reels and it is supported by a range of guiding elements such as fixed-guides, rollers, air-reversers, coating nozzles, driers, etc. It is well known that during processing the web unavoidably deviates from its prescribed, linear path. The lateral web dynamics can be due to roller tilt, web defects, reel wobble and other factors. One of the key factors in understanding the effects of such imperfections on lateral web dynamics has been mechanistic modeling of the web transport process. In particular, mechanics of a translating web interacting with a roller has been the subject of several critical works.

Shelton, and Shelton and Reid (SR) showed that the lateral web deflections can be modeled by using the beam theory, and they described the mechanics of

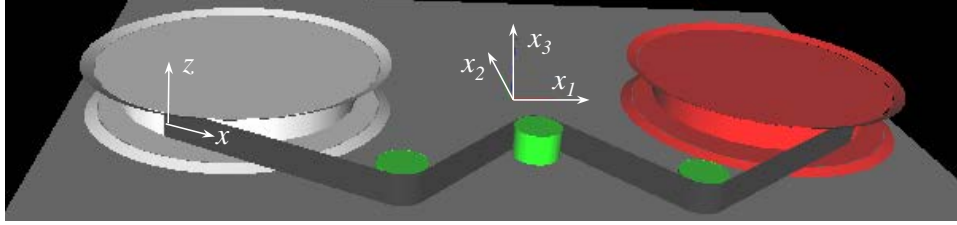


Figure 1 – Schematic depiction of the tape coordinate system (x, z) and the drive base coordinate system (x_1, x_2, x_3) .

The web as it comes into contact with a cylindrical roller [1]. Their work, which describes the web dynamics in the free span between two rollers, was the first to identify the boundary conditions between the web and the downstream roller. Sievers extended this work to a system with multiple rollers and used the Timoshenko beam theory [2]. Benson obtained the downstream boundary conditions by using the minimum total potential energy principle, and described the mechanics of a spliced web by using the Timoshenko beam theory [3]. In the limit when Euler-Bernoulli and Timoshenko beam models are identical the boundary conditions described by SR and Benson are identical. The aforementioned works do not directly model the interaction of a web with a roller. Mechanics of a string travelling over a cylindrical roller was described by Ono [4] and Moustafa [5]. Raeymaekers et al. [6] extended Ono's model by adding the effects of bending stiffness [7]. However, these models have not considered systems with multiple rollers, and they don't take into account the roller misalignment. Brake and Wickert [8, 9] introduced a framework where various types of guides on a tape path can be modeled by applying concentrated forces and moments. The present work introduces a general model for modeling the lateral dynamics of a web travelling between two reels, supported by multiple rollers.

MODEL

The positions and orientations of the web path components are described with respect to the fixed coordinate system (x_1, x_2, x_3) placed on the drive base as shown in Figure 1. The reference axis, x , of the web is described by the centerline (neutral-axis) of the web as it wraps around idealized rollers between the supply and take-up reels. The orientation of the spin-axis (x_3) of a *tilted roller* is described by rigid body rotations δ and α with respect to x_1 - and x_3 -axes, respectively, as shown in Figure 2 [8, 10]. The position $w_g(\theta)$ and slope θ_g of the centerline of a tilted roller are described with respect to the x -axis of an idealized tape path, as follows [8, 10],

$$w_g(\theta) = -R \sin \delta \cos \theta \quad \{1\}$$

$$\theta_g(x) = \frac{dw_g}{dx} = \sin \delta \sin \theta \quad \{2\}$$

Note that, in general, the circumferential coordinate θ , around the roller, and the centerline of the web can be related as $x = R\theta$. Figure 3 shows an example of w_g and θ_g variations for a roller with $R = 5$ mm, $\alpha = 0$, $\delta = 1$ mrad and wrap angle of 79 degrees.

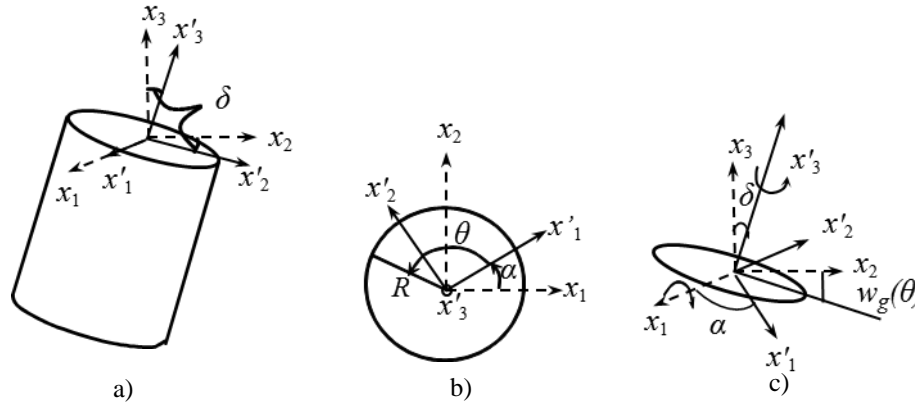


Figure 2 – Definitions of a) the tilt angle δ , b) the orientation angle α , and c) the definition of the change of height $w_g(\theta)$

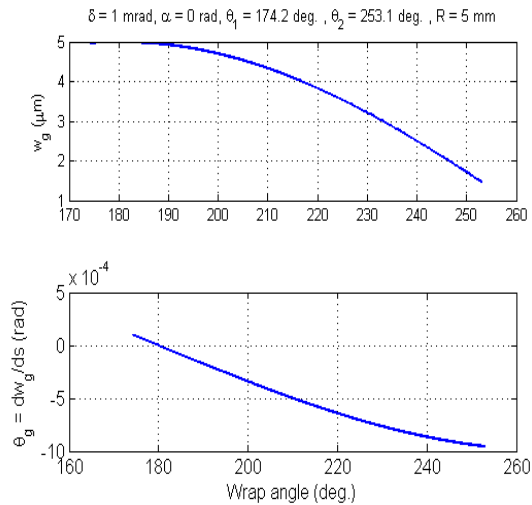


Figure 3 – The deviation of the tape's centerline expressed in the tape's coordinate system. The deviation is indicated by w_g and the slope of the deviation is indicated by θ_g .

In case there is sufficient traction between the roller and the web and negligible bearing loss on the roller axis, no-slip will take place in the interface and the web transport speed V_x will be equal to the rotational speed of the guide ΩR . In case the roller axis deviates from the ideal as described above, Shelton observed that frictional moments develop between the web and the roller and adjust the web path to satisfy the velocity matching condition. A direct result of this is that "every point on the web which is in or

immediately upstream of the contact area of a cylindrical roller moves perpendicularly to roller” [11]. As the web contacts the downstream roller located at $x = L$ the boundary conditions described by SR are expressed follows,

$$\text{at } x = L: \quad \frac{\partial w}{\partial t} + V_x \frac{\partial w}{\partial x} = V_x \delta(t) \quad \text{and} \quad \frac{\partial^2 w}{\partial t^2} = V_x^2 \frac{\partial^2 w}{\partial x^2} \quad \{3\}$$

The first relationship represents the velocity matching condition for the web centerline and the second one represents the same condition for the entire width of the web [3].

In this paper, a “stick” condition which allows the web to follow the centerline of the roller is implemented. The slip condition that that can cause harmful dynamics, particularly in the data-tape recording application as reported by Yang and Müftü [12], is not considered in this paper.

The model considers the following effects on the lateral dynamics of the web. The web path consists of numerous rollers a supply reel and a take-up reel, e.g. Figure 1. The spin-axis of a given roller can be tilted with respect to the drive base. The web can move laterally over the roller surface, and its final position will depend on the up/downstream conditions provided by the web. It is assumed that the lateral dynamics of the web can be modeled by using the translating beam mechanics based on Euler-Bernoulli beam theory. It is also assumed that in the longitudinal direction, no gross-slip such as the one that occurs over fixed guides takes place. Moreover, the effects of local slip are neglected in this first order model. Therefore, the web tension is assumed to remain constant over a roller. Finally, it is assumed that as the web wraps around a roller, it primarily sticks to the roller surface.

The equation of lateral web motion for a web interacting with multiple rollers is then given as follows [8, 9],

$$\rho \frac{D^2 w}{Dt^2} + EI \frac{\partial^4 w}{\partial x^4} - \frac{\partial}{\partial x} \left(T \frac{\partial w}{\partial x} \right) + \sum_{i=1}^{N_r} H_i k \left(\frac{\partial w}{\partial x} - \theta_{g_i} \right) = \sum_{i=1}^{N_r} H_i \left(\frac{T}{R_i} \cos \theta_{g_i} \sin \delta_i \right) \quad \{4\}$$

where the subscript i refers to a particular roller on the web path whose position, tilt angles, δ_i , α_i , radius R_i , and wrap angle θ_{wi} are known, N_r represents the number of rollers, H_i is a windowing function that is equal to 1 over a roller and 0 anywhere else. The first three terms of this equation represent the inertial forces, the restoring forces due to bending and the restoring force due to tension, respectively. Since the web is translating with a constant velocity V_x and the equilibrium is expressed in a space fixed reference frame, material time derivative is used in calculating the acceleration due to lateral web motion.

The fourth term of Equation {4}, which involves the constant foundation stiffness parameter k , is introduced over the rollers in order to impose the slope matching condition. The unit of k is N.m/rad and it represents a discontinuous elastic foundation, which acts on the slope of the web. Note that as the web slope matches the guide slope θ_g the net effect of this term is zero. Thus this term provides the function of the boundary conditions as described by Shelton and Reid. The last term in Equation {4} is due to lateral component of belt-wrap pressure [8, 10].

In order to model the web dynamics between two reels we only need two boundary conditions at the supply and take-up reels located at $x = 0$ and L . Brake describes the

boundary conditions in case the supply pack axis is not perfectly aligned. In this case the position and slope of the web coming off of the supply reel are given as follows,

$$\text{at } x = 0: \quad w = d_0 + R_0\psi_{0s} \quad \text{and} \quad \frac{\partial w}{\partial x} = \psi_{0s} \quad \{5\}$$

where d_0 is the linear offset of the axis, ψ_0 is the tilt of the reel axis described similar to the roller imperfection, and R_0 is the radius of the web coming off the reel. On the take-up reel side, at $x = L$, the web velocity and slope match the take-up reel's velocity and slope as follows,

$$\text{at } x = L: \quad \frac{Dw}{Dt} = V_x\psi_L \quad \text{and} \quad \frac{D}{Dt} \left(\frac{\partial w}{\partial x} \right) = V_x\dot{\psi}_L \quad \{6\}$$

where ψ_L

Equations {4} - {6} are solved numerically. Spatial discretization is achieved by the finite element method. Time integration is carried out by Newmark's method.

RESULTS AND DISCUSSION

Comparison of the Models

In order to compare the model presented in this paper to the SR-model the steady state lateral deflection of the single roller system shown in Figure 4 is analyzed with the baseline parameters given in Table 1. In the case of the SR-model, the domain of analysis is the free span between two rollers ($0 \leq x \leq L_1$). The web is assumed to be leaving the upstream roller ($x = 0$) in a perfect manner with zero lateral deflection and slope. The roller, at $x = L_1$, is tilted by δ ; the corresponding boundary conditions are given in Equation {3}. The solution for the SR-model is obtained by using the method described by Sievers [2] for the case of a tensioned Euler-Bernoulli beam.

In the case of the present model, the domain of analysis is ($0 \leq x \leq L_1+L_2+L_3$). The roller in question is located in the region ($L_1 \leq x \leq L_2$). The web is assumed to leave the first roller ($x = 0$) perfectly and enter the last roller likewise $x = (L_1+L_2+L_3)$. Therefore, for this comparison, the web slope and displacement are set to zero at $x = 0$ and ($L_1+L_2+L_3$). Solution is obtained by solving Equation {4} numerically.

Effects of the Downstream Web Span Length and the Wrap Angle

First, the effect of the free-span, L_3 , on the equilibrium position of the web is investigated. The upstream length, L_1 , the wrap-angle, θ_w , and web thickness, h , are fixed as 0.42 m, 45° and 0.2 mm respectively. L_3 values are varied between 0.41 m and 11.07 m, as shown in Figure 5. The new model approaches the SR-model as L_3 increases. For this case increasing L_3 beyond 6.73 m, does not change the web position, any further. However, improvement in the predictions can be achieved if the upstream and the downstream web segments can be effectively isolated from one another. One way to enable this is to increase the wrap angle. The effects of the wrap angle θ_w on the web position are shown in Figure 5b for $L_1 = 0.42$ and $L_3 = 6.73$ m. This shows that as the wrap angle is increased two solutions approach one another, indicating that increasing wrap angle play a crucial role in isolating the effects of the restoring forces on the upstream and downstream sides.

In general, a shorter span of web is expected to be stiffer. In the case of $L_3 = 0.41$ m the restoring forces and moments from the downstream side have significant effects on the equilibrium position of the upstream side. However, as the length of the downstream span is increased the restoring forces and moments applied by the relatively more compliant downstream span is no longer sufficient to affect the upstream mechanics of the web. Therefore, the predictions of the two models become closer to one another.

Effects of the Upstream Web Span Length

A similar analysis is carried out to investigate the effects of the upstream span-length, L_1 , on the equilibrium position of the web, for fixed downstream span-lengths L_3 . L_1 is varied in the range of 0.4 – 1.7 m, for a relatively short and a relatively long value of L_3 in Figures 6a and 6b, respectively. The predictions of the SR-model are plotted as solid lines. In the case of $L_3 = 0.52$ m (Figure 6a) the upstream span has a very strong influence on the equilibrium position of the web and the two models do not match well. This is especially more significant for the longer web spans on the upstream side. The case $L_1 = 1.37$ m shows a significant deviation from SR-model, but as the length of the upstream span becomes comparable to that of the downstream span the two modeling approaches predict similar results.

In the case of $L_3 = 6.67$ m (Figure 6b) the upstream span has a relatively lower, but still non-negligible, influence on the equilibrium position of the web on the roller. As in the previous case, by choosing increasingly shorter and thus stiffer upstream span-lengths, the deviations become smaller. These observations are consistent with the previous section.

Simulation of a Weave Imperfection through a Four-Roller Web Path

Due to manufacturing tolerances, the strain free-state of the web could be non-straight, affecting the lateral deflection of the web during transport. Benson [3] and Brake [8] expressed the shape of the imperfection as $w_0(x, t) = A_w \sin(2\pi(x - V_x t)/\lambda_w)$ with amplitude A_w and wavelength λ_w . Such an imperfection would travel in the downstream direction with velocity V_x and would cause a “weave” motion of the web, even if the web leaves the supply roller perfectly.

The layout shown in Figure 7 is used to as a platform to simulate the web weave, with the variables quantified in Table 1. Figure 8 shows snapshots of the web deflection and slope profiles, moving through the path which consists of four ideal rollers, a supply reel located at $x = 0$ position, and a take-up reel at $x = L = 9.35475$ m. The roller positions are marked with symbols ‘oo’ on the horizontal axis. Figures 9a and 9b show the web deflection and slope histories for a full period ($T = V_x/\lambda_w$) during the state of steady motion. The lateral deflection of the web is symmetrical with respect to the idealized centerline. The amplitude of weave experienced over the path never reaches the full amplitude $A_w = 5$ mm, however, the lateral web deflection grows as the web moves downstream. The largest lateral web deflection amplitude occurs over the take-up roller. This would cause a scatter-wind, if left uncorrected.

It is seen that the web approaches each roller perpendicularly as the weave moves through the system, while the lateral position of the web over each roller is adjusted to keep the overall force and moment balance of the entire system. Clearly, the lateral motion over the roller of the scale shown here would come with some amount of lateral sliding. The effects of these sliding forces on the web dynamics are not considered in this paper, but will be included in a future work.

Figure 9 shows, a simulation of the web weave over the same path, with slightly imperfect rollers. The axes of the rollers 1 and 2 are tilted by $\delta = 1$ mrad, and rollers 3 and 4 by -1 mrad. The α -parameter is zero for all four rollers. The general response of the web over this path is similar. Clearly the lateral deflection is no longer symmetrical with respect to the ideal centerline, and the web prefers to wind toward the left side of the downstream direction on the take-up roller. The model preserves the normal approach angle between the roller and the web, and the web is able to follow the contour of the centerline of the roller.

SUMMARY AND CONCLUSIONS

A model for simulating the lateral web dynamics over a group of rollers is presented. The model consists of a single partial differential equation with discontinuous elastic foundations acting on the slope of the web deflection over the rollers. The mechanics of the web-to-roller interactions is based on the Shelton and Reid (SR) model where the web is forced to follow the contour of the roller, and thus preserve the ninety-degree entry rule. The results of the model are compared to the SR-model for a single roller system. In general, good agreement between the two models is shown when the upstream and downstream lengths of the web are relatively compliant (long), and when the wrap angle over the roller is relatively large. On the other hand, the present model predicts that the downstream and upstream web mechanics can be coupled to one another due to the restoring force and moments generated in each span. In case the coupling is strong, the lateral deflection of the web deviates from that predicted by SR-model, but the ninety-degree rule is preserved.

The model presented in this paper is sufficiently versatile to simulate the system response for various imperfections. In order to demonstrate this capability the motion of a web with weave imperfection through a layout with four rollers is simulated. This simulation showed that such an imperfection would cause a scatter wind in the take-up roller with amplitude somewhat smaller than the amplitude of the weave imperfection. In case the rollers are tilted the scatter wind is skewed in the axial direction of the take-up reel.

ACKNOWLEDGMENTS

This work has been supported in part by the Information Storage Industry Consortium (INSIC). This work is built upon the simulation platform LTMSim, initially developed by Professor Jonathan A. Wickert and his group of students.

REFERENCES

1. Shelton, J. J. and Reid, K. N. "Lateral Dynamics of an Idealized Moving Web," Journal of Dynamic Systems, Measurement, and Control, Vol. 93, No. 3, 1971, pp. 187-192.
2. Sievers, L. A., Modeling and Control of Web Conveyance Systems, PhD Thesis, 1987, Rensselaer Polytechnic Institute: Troy, New York.
3. Benson, R.C., "Lateral Dynamics of a Moving Web With Geometrical Imperfection," Journal of Dynamic Systems, Measurement, and Control, Vol. 124, No. 1, 2002, pp. 25.
4. Ono, K., "Lateral Motion of an Axially Moving String," Journal of Applied Mechanics, Vol. 46, 1979, pp. 905-912.

5. Moustafa, M., "The Behavior of Threads over Rotating Rolls," Journal of Engineering Sciences, No. 1, Vol. 2, 1975, pp. 37-43.
6. Yang, R.-J., "Steady Motion of a Thread over a Rotating Roller," Journal of Applied Mechanics, No. 61, 1994, pp. 16-22.
7. Raeymaekers, B. and Talke, F. E., "Lateral Motion of an Axially Moving Tape on a Cylindrical Guide Surface," Journal of Applied Mechanics, Vol. 74, No. 5, 2007, pp. 1053.
8. Brake, M. R. W., Lateral Vibration of Moving Media with Frictional Contact and Nonlinear Guides, PhD Thesis, 2007, Carnegie Mellon University: Pittsburgh, PA 15213.
9. Brake, M. R. and Wickert, J. A. "Frictional Vibration Transmission from a Laterally Moving Surface to a Traveling Beam," Journal of Sound and Vibration, Vol. 310, No. 3, 2008, pp. 663-675.
10. Eaton, J. H., "Behavior of a tape path with imperfect component," Adv. Info. Storage Syst., Vol. 8, 1998, pp. 77-92.
11. Shelton, J. J., Lateral Dynamics of A Moving Web, 1968, PhD Thesis, Oklahoma State University.
12. Yang., H. and Müftü, S. "Lateral Tape Dynamics over Non-Linear Guides," in Proceedings of the ASME-ISPS /JSME-IIP Joint International Conference on Micromechatronics for Information and Precision Equipment, MIPE2012: Santa Clara, California, USA.

	Figs. 5-6	Figs. 8-9
	3.50	3.50
v	0.45	0.45
h (mm)	0.2	0.2
b (mm)	250.0	250.0
$R_{i=1}$ (m)	0.18	0.075
$R_{i=2}$ (m)	NA	0.075
$R_{i=3}$ (m)	NA	0.075
$R_{i=4}$ (m)	NA	0.075
R_{reels} (m)	NA	0.18
T (N)	87.5	25
V_x (m/s)	12.5	12.5
ρ (kg/m ³)	1400	1400
α (rad)	0	0
$\delta_{i=1}$ (mrad)	1	1
$\delta_{i=2}$ (mrad)	NA	1
$\delta_{i=3,4}$ (mrad)	NA	-1
A_w (mm)	NA	5
λ_w (m)	NA	10

Table 1 – Parameters used in this work.

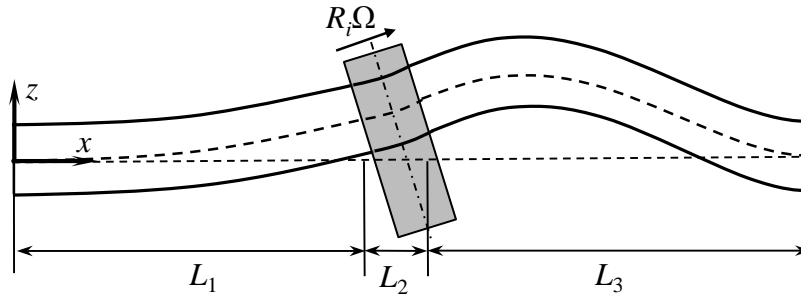


Figure 4 – Schematic depiction of the system used to compare the SR-model with the present model. The upstream length is L_1 , the wrap length is L_2 , and the downstream length is L_3 with roller radius $R=0.18$ m.

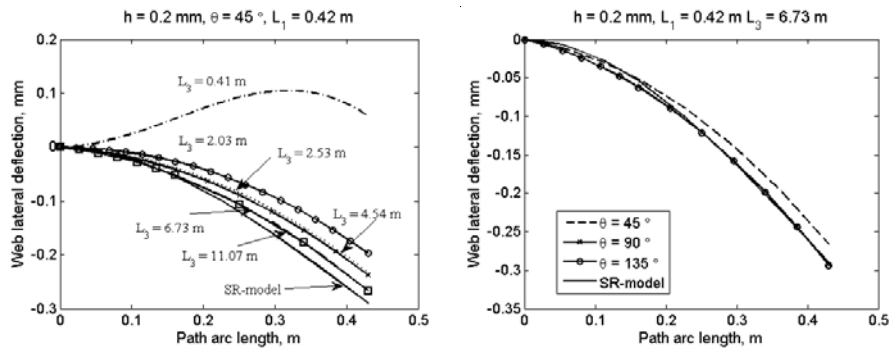


Figure 5 – a) The effects of downstream free-span length, L_3 , on the lateral position of the web at steady state. $L_1 = 0.42$ m, $\theta_w = 45^\circ$. b) The effects of the wrap angle, θ_w , on the lateral position of the web at steady state. $L_1 = 0.42$ m, $L_3 = 6.73$ m.

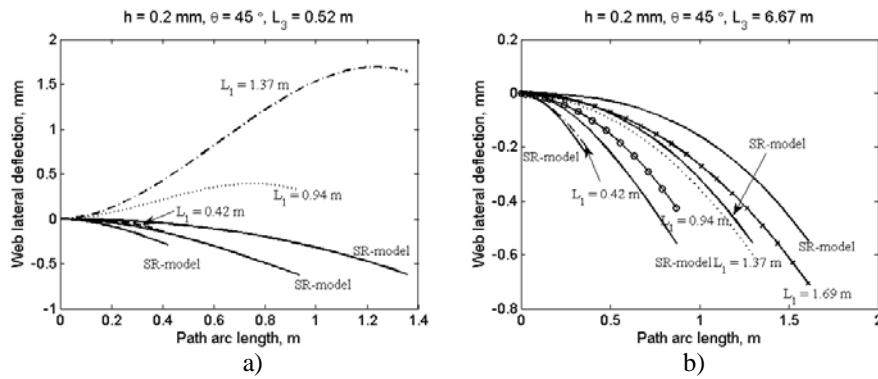


Figure 6 – a) The effects of upstream free-span length, L_1 , on the lateral position of the web at steady state. a) $L_3 = 0.52$ m, b) $L_3 = 6.67$ m.

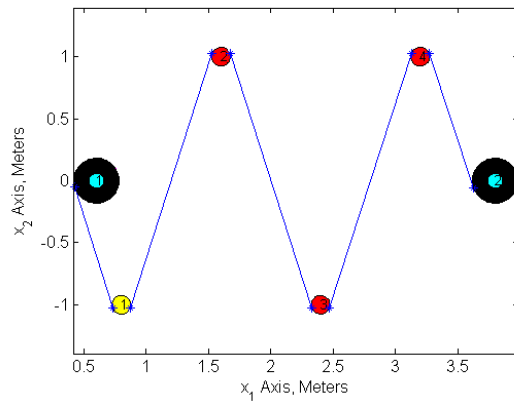


Figure 7 – The path which consist of four rollers and two reels used in the simulations (Figs. 8 and 9). Parameters defined in Table 1.

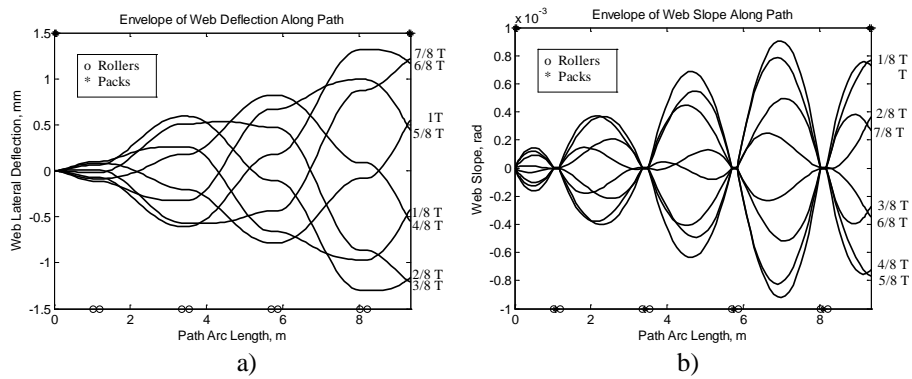


Figure 8 – Web response to a web with weave imperfection. a) Lateral web deflection, b) slope of lateral deflection during one period. The four rollers are ideally aligned in the path shown in Figure 7.

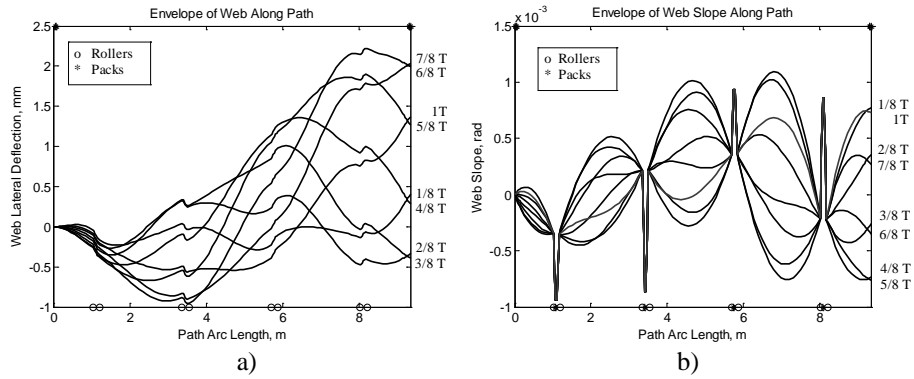


Figure 9 – Web response to a web with weave imperfection. a) Lateral web deflection, b) slope of lateral deflection during one period. The four rollers in the path shown in Figure 7 have misalignments as defined in Table 2.